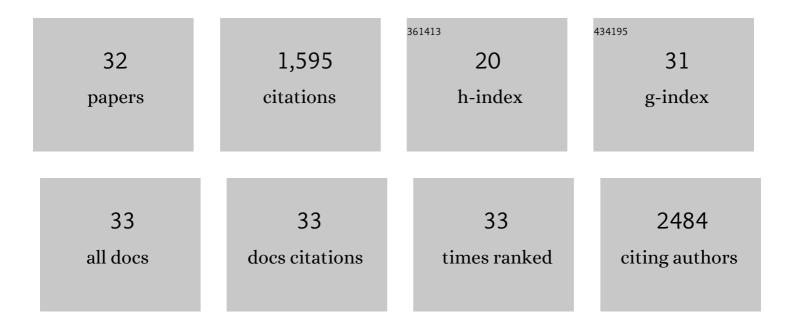
Ping-Chang Lin

List of Publications by Year in descending order

Source: https://exaly.com/author-pdf/7620980/publications.pdf Version: 2024-02-01



#	Article	IF	CITATIONS
1	Manganese-enhanced magnetic resonance imaging method detects age-related impairments in axonal transport in mice and attenuation of the impairments by a microtubule-stabilizing compound. Brain Research, 2022, 1789, 147947.	2.2	1
2	Glucocorticoid-Induced Leucine Zipper Promotes Neutrophil and T-Cell Polarization with Protective Effects in Acute Kidney Injury. Journal of Pharmacology and Experimental Therapeutics, 2018, 367, 483-493.	2.5	19
3	CXCR2-Expressing Tumor Cells Drive Vascular Mimicry in Antiangiogenic Therapy–Resistant Glioblastoma. Neoplasia, 2018, 20, 1070-1082.	5.3	54
4	Repeated exposures to diisopropylfluorophosphate result in structural disruptions of myelinated axons and persistent impairments of axonal transport in the brains of rats. Toxicology, 2018, 406-407, 92-103.	4.2	24
5	Predicting early symptomatic osteoarthritis in the human knee using machine learning classification of magnetic resonance images from the osteoarthritis initiative. Journal of Orthopaedic Research, 2017, 35, 2243-2250.	2.3	70
6	Major Challenges and Potential Microenvironment-Targeted Therapies in Glioblastoma. International Journal of Molecular Sciences, 2017, 18, 2732.	4.1	26
7	Multiparametric Classification of Skin from Osteogenesis Imperfecta Patients and Controls by Quantitative Magnetic Resonance Microimaging. PLoS ONE, 2016, 11, e0157891.	2.5	4
8	Sensitivity and specificity of univariate MRI analysis of experimentally degraded cartilage under clinical imaging conditions. Journal of Magnetic Resonance Imaging, 2015, 42, 136-144.	3.4	8
9	Classification of histologically scored human knee osteochondral plugs by quantitative analysis of magnetic resonance images at 3T. Journal of Orthopaedic Research, 2015, 33, 640-650.	2.3	13
10	Assessment of chemical exchange in tryptophan–albumin solution through 19F multicomponent transverse relaxation dispersion analysis. Journal of Biomolecular NMR, 2015, 62, 121-127.	2.8	5
11	Nuclear Magnetic Resonance Spectroscopy in Nanomedicine. Progress in Optical Science and Photonics, 2015, , 59-84.	0.5	2
12	Prediction of cartilage compressive modulus using multiexponential analysis of <i>T</i> ₂ relaxation data and support vector regression. NMR in Biomedicine, 2014, 27, 468-477.	2.8	4
13	Techniques for physicochemical characterization of nanomaterials. Biotechnology Advances, 2014, 32, 711-726.	11.7	497
14	Comparison of visceral fat measured by magnetic resonance imaging and dualâ€energy Xâ€ray absorptiometry in women. FASEB Journal, 2013, 27, 852.9.	0.5	0
15	Infrared Fiber Optic Probe Evaluation of Degenerative Cartilage Correlates to Histological Grading. American Journal of Sports Medicine, 2012, 40, 2853-2861.	4.2	36
16	Cockayne syndrome group B protein prevents the accumulation of damaged mitochondria by promoting mitochondrial autophagy. Journal of Experimental Medicine, 2012, 209, 855-869.	8.5	177
17	Characterization of Engineered Cartilage Constructs Using Multiexponential <i>T</i> ₂ Relaxation Analysis and Support Vector Regression. Tissue Engineering - Part C: Methods, 2012, 18, 433-443.	2.1	15
18	Multivariate analysis of cartilage degradation using the support vector machine algorithm. Magnetic Resonance in Medicine, 2012, 67, 1815-1826.	3.0	31

PING-CHANG LIN

#	Article	IF	CITATIONS
19	Improved MRâ€based characterization of engineered cartilage using multiexponential <i>T</i> ₂ relaxation and multivariate analysis. NMR in Biomedicine, 2012, 25, 476-488.	2.8	28
20	Cockayne syndrome group B protein prevents the accumulation of damaged mitochondria by promoting mitochondrial autophagy. Journal of Cell Biology, 2012, 197, i4-i4.	5.2	0
21	Mapping proteoglycanâ€bound water in cartilage: Improved specificity of matrix assessment using multiexponential transverse relaxation analysis. Magnetic Resonance in Medicine, 2011, 65, 377-384.	3.0	44
22	Improved specificity of cartilage matrix evaluation using multiexponential transverse relaxation analysis applied to pathomimetically degraded cartilage. NMR in Biomedicine, 2011, 24, 1286-1294.	2.8	30
23	Magnetic Resonance Studies of Macromolecular Content in Engineered Cartilage Treated with Pulsed Low-Intensity Ultrasound. Tissue Engineering - Part A, 2011, 17, 407-415.	3.1	15
24	XRCC1 haploinsufficiency in mice has little effect on aging, but adversely modifies exposure-dependent susceptibility. Nucleic Acids Research, 2011, 39, 7992-8004.	14.5	25
25	Nondestructive Assessment of Engineered Cartilage Constructs Using Near-Infrared Spectroscopy. Applied Spectroscopy, 2010, 64, 1160-1166.	2.2	61
26	Multicomponent T ₂ relaxation analysis in cartilage. Magnetic Resonance in Medicine, 2009, 61, 803-809.	3.0	149
27	Sensitivity and specificity of univariate MRI analysis of experimentally degraded cartilage. Magnetic Resonance in Medicine, 2009, 62, 1311-1318.	3.0	31
28	Classification of degraded cartilage through multiparametric MRI analysis. Journal of Magnetic Resonance, 2009, 201, 61-71.	2.1	46
29	Determination of myoglobin concentration in blood-perfused tissue. European Journal of Applied Physiology, 2008, 104, 41-48.	2.5	31
30	Blood flow and metabolic regulation in seal muscle during apnea. Journal of Experimental Biology, 2008, 211, 3323-3332.	1.7	54
31	Anisotropy and Temperature Dependence of Myoglobin Translational Diffusion in Myocardium: Implication for Oxygen Transport and Cellular Architecture. Biophysical Journal, 2007, 92, 2608-2620.	0.5	38
32	Myoglobin translational diffusion in rat myocardium and its implication on intracellular oxygen transport. Journal of Physiology, 2007, 578, 595-603.	2.9	52